Path Optimization with Application to Tunneling

Dóróthea M. Einarsdóttir, Andri Arnaldsson,
Finnbogi Óskarsson, and Hannes Jónsson

Science Institute, VR-III, University of Iceland, 107 Reykjavík, Iceland

Abstract. A method is presented for optimizing paths on high dimensional surfaces, i.e. scalar functions of many variables. The method involves optimizing simultaneously the end points and several intermediate points along the path and thus lends itself well to parallel computing. This is an extension of the nudged elastic band method (NEB) which is frequently used to find minimum energy paths on energy surfaces of atomic scale systems, often with several thousand variables. The method is illustrated using 2-dimensional systems and various choices of the object function, in particular (1) path length, (2) iso-contour and (3) quantum mechanical tunneling rate. The use of the tunneling paths to estimate tunneling rates within the instanton approximation is also sketched and illustrated with an application to associative desorption of hydrogen molecule from a copper surface, a system involving several hundred degrees of freedom.

Keywords: optimal paths, transitions, instantons.

1 Introduction

There can be several reasons for wanting to find a path on a surface that is optimal in some sense. Our motivation comes mainly from the need to find minimum energy paths (MEPs) on energy surfaces to estimate rates of transitions due to thermally activated, classical trajectories [1], or - as is the focus here - quantum mechanical tunneling through energy barriers [2]. The method used for the path optimization is, however, quite general and can be used in various contexts.

The surface is described by a continuously differentiable function, V, of N variables

$$V : \mathbb{R}^N \rightarrow \mathbb{R} \tag{1}$$

In typical applications to transition rates in atomic scale systems, N is on the order of 10^3. We assume that the gradient ∇V of the object function can be evaluated readily, but second derivatives are not needed. The goal is to find a finite path on the surface that is optimal in some sense. For example, the MEP on an energy surface can be of interest since the point of highest energy on the path, a first order saddle point, gives the activation energy barrier for going from one local minimum to another and, thereby, determines the exponential dependence of the rate on temperature [3,4]. At every point on a MEP

K. Jónasson (Ed.): PARA 2010, Part II, LNCS 7134, pp. 45–55, 2012.

$$\nabla V - \nabla V \cdot \widehat{\tau}\,\widehat{\tau} \;=\; 0 \tag{2}$$

were $\widehat{\tau}$ is the unit tangent vector for the path at that point [5]. Furthermore, the curvature for all modes perpendicular to the path must be positive. The NEB is frequently used to find MEPs for estimating rates of thermal transitions in atomic scale systems where the atoms are described by classical dynamics [5,6]. Some systems have even included over a hundred thousand coordinate variables [7]. The path optimization method presented here is a generalization of the NEB method and can be used, for example, to calculate rates of thermal transitions in quantum mechanical systems were tunneling takes place.

Let $\mathbf{R}$ denote a vector of N variables and $V(\mathbf{R})$ the surface. The object function, $\tilde{S}$, can be defined as a functional of the path, $\mathbf{R}(s)$ where $s \in [0,1]$, that is $\tilde{S} = \tilde{S}[\mathbf{R}(s)]$. The object function can, for example, involve an integral over the path

$$\tilde{S}[\mathbf{R}(s)] = \int_{\mathbf{R}_0}^{\mathbf{R}_n} f(V(\mathbf{R}))d\mathbf{R} \tag{3}$$

where f is some function. The path will be represented by a set of discrete points along the path $\{\mathbf{R}_0, \mathbf{R}_1, \ldots \mathbf{R}_n\}$ and the integral approximated using, for example, the trapezoidal rule. The task is then to find the values of the vectors $\mathbf{R}_i$ that minimize the object function for discretized paths

$$\begin{aligned}\tilde{S}[\mathbf{R}(s)] &\approx S(\mathbf{R}_0, \ldots \mathbf{R}_n) = \\ &= \frac{1}{2}\sum_{i=1}^{n} \left(f(V(\mathbf{R}_i)) + f(V(\mathbf{R}_{i-1}))\right) |\mathbf{R}_i - \mathbf{R}_{i-1}|\end{aligned} \tag{4}$$

There are $n-1$ discretization points representing the path between the two end points, $\mathbf{R}_0$ and $\mathbf{R}_n$, which can be constrained to have some predetermined values of V, i.e. $V(\mathbf{R}_0) = v_a$ and $V(\mathbf{R}_n) = v_b$. In the NEB, end points of the path are fixed (usually at minima), but in this more general formulation the position of the end points is adjusted during the optimization along the iso-contours corresponding to v_a and v_b.

2 Path Optimization

The optimization is started by specifying some trial set of discretization points $\{\mathbf{R}_0^0, \mathbf{R}_1^0, \ldots \mathbf{R}_n^0\}$ and then iterating until $S(\mathbf{R}_0, \mathbf{R}_1, \ldots \mathbf{R}_n)$ has reached a minimum value. Let the negative gradient of the functional, S, with respect to the discretization point, $\mathbf{R}_j$, be denoted by

$$\mathbf{g}_j = -\nabla_j S \tag{5}$$

This represents the direction of steepest descent for each one of the discretization points and can be used in a minimization algorithm to find the set of vectors $\{\mathbf{R}_0, \mathbf{R}_1, \ldots \mathbf{R}_n\}$ that minimize S. But, only the component of $\mathbf{g}_j$ that is perpendicular to the path should be included in the optimization [1,6]. The distribution

of the discretization points along the path is controlled separately and should not be affected by S. This projection is referred to as 'nudging'. The negative gradient, $\mathbf{g}_j$, is projected along the path

$$\mathbf{g}_j^{\parallel} = (\mathbf{g}_j \cdot \widehat{\tau}_j)\widehat{\tau}_j \tag{6}$$

and the rest of the vector is the perpendicular component

$$\mathbf{g}_j^{\perp} = \mathbf{g}_j - \mathbf{g}_j^{\parallel} \ . \tag{7}$$

The discretization points can be distributed along the path in various ways, for example by using a restraint method where a 'spring' acting between adjacent discretization points is added, Again, a projection is used to make sure this does not affect the location of the converged path. For the discretization points that are not at the ends, $\{\mathbf{R}_1, \mathbf{R}_2, \ldots \mathbf{R}_{n-1}\}$, the component of $\mathbf{g}_j$ parallel to the path is replaced by

$$\mathbf{g}_j^{sp} = k\left(|\mathbf{R}_{j+1} - \mathbf{R}_j| - |\mathbf{R}_j - \mathbf{R}_{j-1}|\right)\widehat{\tau}_j \tag{8}$$

where k is analogous to a spring constant. A wide range of values can be chosen for k without affecting the results, but the convergence rate is in general faster if the $\mathbf{g}_j^{sp}$ are roughly of the same magnitude as the $\mathbf{g}_j$. The total $\mathbf{g}$ that is used in the optimization is then given by the vector sum

$$\mathbf{g}_j^{\text{opt}} = \mathbf{g}_j^{\perp} + \mathbf{g}_j^{sp} \tag{9}$$

for $j = 1, \ldots, n-1$. In a steepest descent algorithm, all the discretization points $\mathbf{R}_j$ will be displaced in the direction of $\mathbf{g}_j^{\text{opt}}$ at each iteration. A more efficient approach is discussed in section 2.1. If the spring constant, k, is the same for all pairs of adjacent discretization points, then the points will be equally spaced along the path when convergence has been reached. If a different distribution is desired, the values of k for each adjacent pair of discretization points can be chosen accordingly.

The steepest descent direction for the end points is defined differently since they should only move along the iso-contours corresponding to v_a or v_b. The component of $\mathbf{g}^{sp}$ parallel to the gradient of V needs to be zeroed so the end points only get displaced along the iso-contour. Furthermore, a restraint is added to pull the end points towards the iso-contour if curvature has resulted in a drift away from the iso-contour. Denoting the unit vector in the opposite direction of the gradient of V as

$$\widehat{\mathbf{F}} = -\nabla V/|\nabla V| \tag{10}$$

the steepest descent direction for end point $\mathbf{R}_0$ can be written as

$$\mathbf{g}_0^{\text{opt}} = \mathbf{g}_0^{sp} - \left(\mathbf{g}_0^{sp} \cdot \widehat{\mathbf{F}}_0 - V(\mathbf{R}_0) + v_a\right)\ \widehat{\mathbf{F}}_0 \tag{11}$$

where

$$\mathbf{g}_0^{\text{sp}} = k\ (\mathbf{R}_1 - \mathbf{R}_0 - \ell\ \widehat{\mathbf{F}}_0) \tag{12}$$

and $\widehat{\mathbf{F}}_0 = \widehat{\mathbf{F}}(\mathbf{R}_0)$. Here, the parameter ℓ has been introduced to make it possible to adjust the length of the path when the endpoints are not constrained (for example, in the iso-contour example below). If ℓ is chosen to be $\ell = L/n$ the path will have length L when the endpoints are free to move during the optimization. An analogous expression holds for the other end point, $\mathbf{R}_n$

$$\mathbf{g}_n^{\text{opt}} = \mathbf{g}_n^{sp} - \left(\mathbf{g}_n^{sp} \cdot \widehat{\mathbf{F}}_n - V(\mathbf{R}_n) + v_b\right) \widehat{\mathbf{F}}_n \tag{13}$$

where

$$\mathbf{g}_n^{\text{sp}} = k\ (\mathbf{R}_{n-1} - \mathbf{R}_n - \ell\ \widehat{\mathbf{F}}_n). \tag{14}$$

and $\widehat{\mathbf{F}}_n = \widehat{\mathbf{F}}(\mathbf{R}_n)$. $\mathbf{g}_0^{\text{opt}}$ and $\mathbf{g}_n^{\text{opt}}$ give the steepest descent direction for the two end points used in the iterative optimization while equation (9) applies to the intermediate discretization points.

2.1 Optimization of the Path

While the location of the discretization points of the path can be optimized by steepest descent displacements in the direction of $\mathbf{g}^{\text{opt}}$, this tends to have slow convergence and various more efficient minimization algorithms can be employed. We have found it useful to divide this numerical optimization into two phases: an initial phase with a rather conservative algorithm and then a final phase with a quadratically convergent algorithm. In the case of atomic scale systems, such as the H_2/Cu system discussed in section 4, the transition is made when the RMS force has dropped to below 0.5 $eV/\mathring{A}$.

In the beginning, the system can be far from the optimal path. Often, a good guess for the optimal path is not available. A method we have found to be robust and convenient to implement is based on modified classical dynamics where the effective mass associated with each degree of freedom is arbitrarily set to unity and the force is taken to be the steepest descent vector. By introducing a certain damping in the dynamics, convergence to a minimum is obtained. The damping involves zeroing the velocity from previous iteration, except for the component in the direction of the force in the current iteration when the projection of the velocity on the force is positive. This algorithm is explained in ref. [1]. In the second phase, a quadratically convergent algorithm such as conjugate gradients or BFGS is more efficient. Some modifications of these algorithms have to be made, though, because an object function corresponding to the steepest descent direction $\mathbf{g}^{opt}$ is not known. The projection (nudging) and addition of the springs modifies the steepest descent direction in such a way that it no longer corresponds to the gradient of S. A review of several minimization methods proposed for the optimization of elastic bands in the context of minimum energy paths and comparison of their efficiency has recently been published [8]. We expect similar performance for the elastic bands presented here, but systematic performance analysis have not yet been made.

Since the optimization of the paths is carried out by adjusting the location of each one of the discretization points simultaneously, and the calculation of

the steepest descent direction only depends on coordinates of each point and its two nearest neighbors, this algorithm for path optimization lends itself well to parallel computing.

3 Examples

3.1 Example I: Shortest Path between Iso-contours

A simple illustration of the method described above is a search for the shortest path between two iso-contours of a given value $\nu_a = \nu_b = \nu$. Here, f can be chosen to be a constant, $f(V) = 1$, and $\ell = 0$. The object functional is simply

$$S^l(\mathbf{R}_0, \ldots, \mathbf{R}_n) = \sum_{i=1}^{n} |\mathbf{R}_i - \mathbf{R}_{i-1}| \tag{15}$$

Differentiation of S gives

$$\mathbf{g}_j = -\nabla_j S^l = -\frac{\mathbf{R}_j - \mathbf{R}_{j-1}}{|\mathbf{R}_j - \mathbf{R}_{j-1}|} + \frac{\mathbf{R}_{j+1} - \mathbf{R}_j}{|\mathbf{R}_{j+1} - \mathbf{R}_j|} \tag{16}$$

Using the equations (9), (11) and (13) in an iterative optimization scheme, gives points along the path which has the shortest distance between two iso-contours, as illustrated in figure 1.

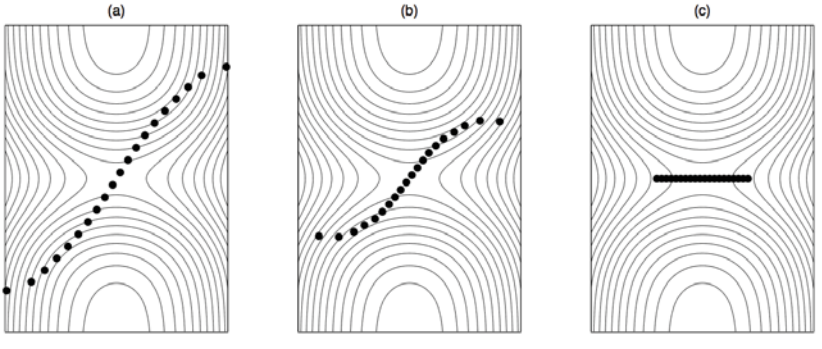

Fig. 1. Path optimization where the object function is the length of the path and the end points are confined to a contour on the surface. (a) Initial path with end points at arbitrary locations on two separate segments the contour; (b) intermediate configuration of the path during the optimization; (c) the final, converged, shortest path between the two contour lines.

3.2 Example II: Tracing Out an Iso-contour

Another example is a path that lies along an iso-contour, say $V = v_c$. Here, f is chosen to be $f(V) = (V - v_c)^2/2$ and $\ell = L/n$ where L is the desired length of the path. The object function becomes

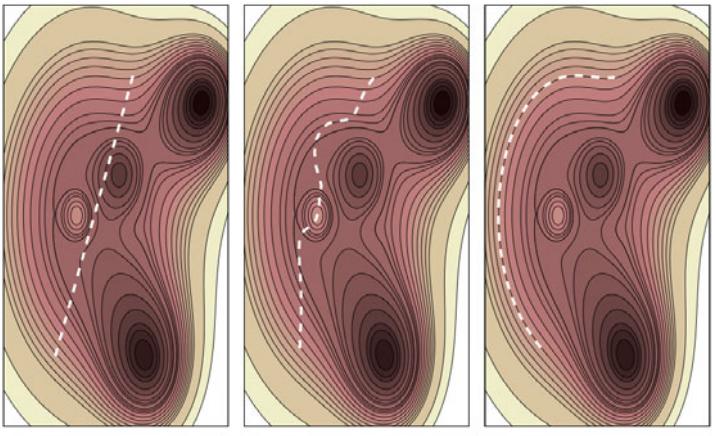

Fig. 2. Path optimization where the object function includes the squared deviation from the contour value. (left) An arbitrary initial path; (middle) intermediate configuration of the path during the optimization; (right) the final, converged path tracing the contour.

$$S^c(\mathbf{R}_0, \ldots \mathbf{R}_n) = \frac{1}{2}\sum_{i=0}^{n}(V(\mathbf{R}_i) - v_c)^2 \;\; |\mathbf{R}_i - \mathbf{R}_{i-1}| \tag{17}$$

Optimization using equations (9), (11) and (13), gives discretization points $\{\mathbf{R_i}\}$ for a path that lies along the v_c iso-contour as is shown in figure 2.

3.3 Example III: Tunneling Path

The optimization procedure described in the previous section can be used to find optimal, quantum mechanical tunneling paths. The function V then represents potential energy of the system and the vector $\mathbf{R}$ consists of the coordinates of all the particles in the system, some of which may undergo a tunneling transition from one position to another. In the path optimization, all particles in the system are allowed to move, unless boundary conditions restricting their movement are applied. In the JWKB method [2], the tunneling path for energy E_c is the path between classical turning points $V(\mathbf{R}_0) = V(\mathbf{R}_n) = E_c$ where the action, S^t, is minimized

$$\tilde{S}^t[\mathbf{R}(s)] = \frac{1}{\hbar}\int_{\mathbf{R}_0}^{\mathbf{R}_n} \sqrt{2\mu(V(\mathbf{R}) - E_c)}d\mathbf{R} \tag{18}$$

Here, μ is the effective mass which is conveniently taken into account by using mass weighted coordinates and forces [9]. The optimization yields a path corresponding to the lowest value of the integral and gives the highest JWKB estimate of the tunneling probability [2,10,11,12]. A reasonable initial guess for the path could be a straight line interpolation between the minima of the initial and final states, but any guess where the end points are placed on different sides of a saddle point higher than E_c will give a tunneling path.

After discretizing the integral, equation (18) becomes

$$S^t(\mathbf{R}_0, \ldots \mathbf{R}_n) = \frac{1}{2\hbar} \sum_{i=1}^{n} \Big(\sqrt{2\mu(V(\mathbf{R}_i) - E_c)} + \sqrt{2\mu(V(\mathbf{R}_{i-1}) - E_c)} \Big) |\mathbf{R}_i - \mathbf{R}_{i-1}| \tag{19}$$

To simplify the notation, it is convenient to define a new function

$$\xi_i = \frac{1}{\hbar} \sqrt{2\mu(V(\mathbf{R}_i) - E_c)} \tag{20}$$

and rewrite the action integral as

$$S^t(\mathbf{R}_0, \ldots \mathbf{R}_n) = \frac{1}{2} \sum_{i=1}^{n} (\xi_i + \xi_{i-1}) |\mathbf{R}_i - \mathbf{R}_{i-1}| \tag{21}$$

Differentiating this expression with respect to the position of the intermediate discretization points $j = 1, \ldots, n-1$, gives

$$\mathbf{g}_j = -\nabla_j S^t = -\frac{1}{2} \left(\frac{\mu}{\hbar \xi_j} (d_j + d_{j+1}) |\nabla V(\mathbf{R}_j)| \widehat{\mathbf{F}}_j - (\xi_j + \xi_{j-1}) \widehat{\mathbf{d}}_j + (\xi_{j+1} + \xi_j) \widehat{\mathbf{d}}_{j+1} \right). \tag{22}$$

where $\widehat{\mathbf{F}}_j$ is again given by equation (10) and the d_j and $\widehat{\mathbf{d}}_j$ are defined as

$$d_j = |\mathbf{R}_j - \mathbf{R}_{j-1}| \tag{23}$$

$$\widehat{\mathbf{d}}_j = (\mathbf{R}_j - \mathbf{R}_{j-1})/d_j \tag{24}$$

The steepest descent direction, $\mathbf{g}^{\text{opt}}$, is given by equation (9) for the intermediate discretization points, but for the end points equation (11) and (13) are used. By iteratively moving the discretization points, the optimal tunneling path can be found, i.e. the values of $\{\mathbf{R}_0, \ldots \mathbf{R}_n\}$ that minimize S^t.

To illustrate how the method works, the tunneling path of a particle subject to the 2-dimensional potential function used in example II was found, starting initially with an arbitrary, straight path. Various stages of the optimization of the path are shown in figure 3: the initial guess, two intermediate paths during the optimization process and the final, optimal tunneling path. Note that the surface has extra minima and maxima which makes the problem somewhat challenging even though only 2 degrees of freedom are included.

Since the wave function decays exponentially in the classically forbidden region, the tunneling path can be displaced from the MEP into a region of higher potential energy if this leads to significant shortening of the path. This 'corner-cutting' can be seen form the converged path in figure 3.

The corner-cutting becomes stronger as the temperature is lowered, as can be seen from another 2-D model calculation shown in figure 4. The lower the temperature is, the further the path moves away from the MEP. This effect is particularly strong when the MEP has large curvature.

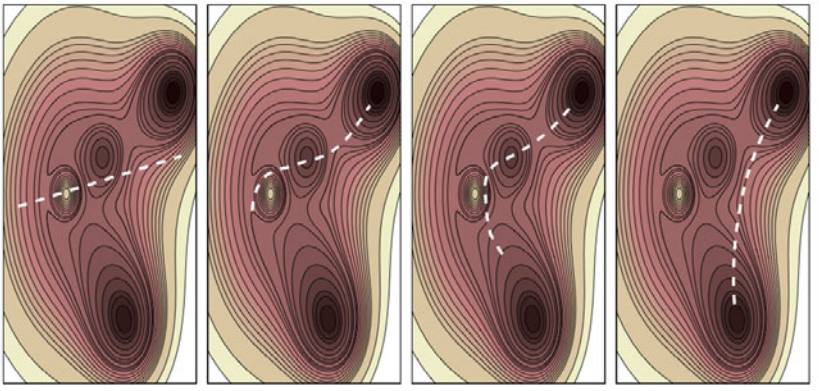

Fig. 3. Path optimization on a surface with an intermediate local minimum and a maximum, starting from an arbitrary straight line path, to illustrate the robustness of the method. Initial path (far left); intermediate paths during the optimization (middle two figures); and converged, optimal JWKB tunneling path (far right).

4 Application: Calculation of Tunneling Rates

The optimal, JWKB tunneling paths discussed in example III above can be used to estimate the tunneling rate at a given temperature rather than at given total energy. The theory is essentially a harmonic quantum transition state theory and is often referred to as 'instanton' theory [10,11]. The path that minimizes the object functional given by equation (18) turns out to be the same as a classical periodic orbit for the inverted potential energy surface , $-V(\mathbf{R})$, and is referred to as the instanton [10]. This is a closed Feynman path and it gives maximum tunneling probability at a temperature which can be related to the period, τ, of the periodic orbit through the relation $T = \hbar/k_B\tau$. The calculation of the period and location of discretization points in the statistical Feynman path corresponding to the optimized JWKB path can be obtained in a rather straight forward way by interpolation between the discretization points. As in harmonic transition state theory, where the reaction rate is estimated by approximating the potential energy surface around the classical saddle point by a quadratic expansion, the quantum mechanical rate can be obtained by expanding the effective quantum mechanical potential energy surface around the instanton to second order [12]. The instanton rate constant, k_{ins}, is given by

$$Q_R \; k_{\text{ins}} = \sqrt{\frac{S_0}{2\pi\hbar}} \; \frac{k_B T P}{\hbar |\prod_j' \lambda_j|} \; e^{-V_{\text{eff}}^{ins}/k_B T} \tag{25}$$

where Q_R is the partition function of the initial state, V_{eff}^{ins} is the value of the effective potential

$$V_{\text{eff}}(\mathbf{R}_0, \ldots \mathbf{R}_n) = \sum_{i=0}^{P} \left[\frac{1}{2} k_{\text{sp}} \, |\mathbf{R}_{i+1} - \mathbf{R}_i|^2 + \frac{V(\mathbf{R}_i)}{P} \right] \tag{26}$$

evaluated at the instanton. Here, P is the number of discretization points in the Feynman path ($\mathbf{R}_{P+1}$ is set equal to $\mathbf{R}_P$) and k_{sp} is the temperature dependent spring constant

$$k_{\mathrm{sp}}(T) = \mu P \left(\frac{k_B T}{\hbar} \right)^2 \tag{27}$$

The λ_j in equation (25) are the frequencies of the normal modes of vibration of the instanton. One vibrational mode has zero eigenvalue, namely the one corresponding to displacement of the images along the path. This mode gives rise to S_0 which is twice the instanton action due to the (imaginary-time) kinetic energy

$$S_0 = \frac{\mu P k_B T}{\hbar} \sum_{j=1}^{P} |\mathbf{R}_j - \mathbf{R}_{j-1}|^2 \tag{28}$$

The prime on the product sign in equation (25) denotes the absence of the zero-mode, since it cannot be treated with a quadratic approximation.

This procedure for estimating the rate constant from JWKB tunneling paths has been tested both on model 2-dimensional systems and for a large system involving several hundred degrees of freedom, the associative desorption of H_2 molecule from a Cu(110) surface. The desorption has been studied by several different methods in the past, including a full free energy method based on Feynman path integrals, the so-called RAW-QTST method [14]. Here, the JWKB paths were used to estimate the desorption rate as a function of temperature using the instanton approximation as described above. The calculation involved 432 degrees of freedom, the coordinates of the two hydrogen atoms and four layers of Cu atoms in a slab subject to periodic boundary conditions. The bottom two layers of Cu atoms in the slab were held fixed. The results are shown in figure 4. The agreement with the full free energy calculation is surprisingly good considering the fact that a gas phase molecule is being formed and that harmonic approximation, which the instanton approach is based on, applies mostly to systems where the effective range of the variables is limited, as is the case for atom coordinates in solids. The instanton approximation involves much less computational effort than RAW-QTST, by about a factor of 10^4, and with the path optimization method presented here, it can be used with atomic forces obtained from electronic structure calculations where each force evaluation can easily take tens of minutes of CPU time. For example, the rate constant for hydrogen atom tunneling in solids has been carried out using the method presented above coupled with density functional theory evaluation of the atomic forces, but those results will be presented elsewhere.

5 Discussion

A general method for finding optimal paths on a multidimensional surface has been presented here. Several two-dimensional problems have been used to illustrate the method, but the strength of the approach is its applicability to

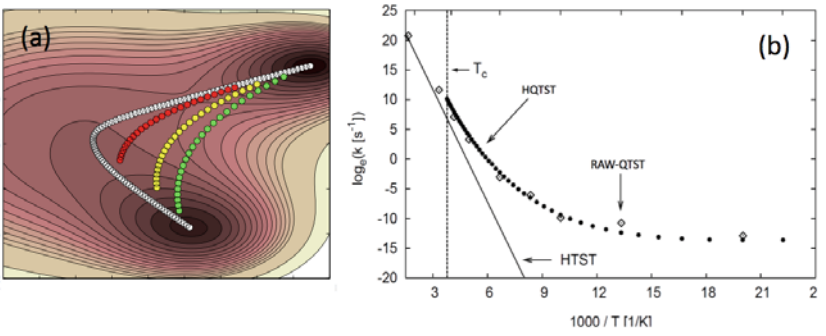

Fig. 4. (a) Model 2-D energy surface with minimum energy path (far left), and converged JWKB tunneling paths for high, intermediate and low (far right) energy. The end points move to the specified system energy. The lower the energy, the more the tunneling path 'cuts the corner', as it moves to a region of higher energy and becomes shorter. (b) Calculation of the rate of H_2 molecule desorption from a Cu(110) surface, including 432 atom coordinates as degrees of freedom. The number of discretization points was $n = 10$ for the highest energy, and $n = 40$ for the lowest energy. The temperature dependence of the rate constant for desorption shows an onset of tunneling at around 250 K. RAW-QTST labels the results from full quantum TST calculation [14]. HQTST labels the results obtained from the instanton approximation, which performs remarkably well here, especially considering that a gas phase molecule is formed.

problems where many, even thousands, of degrees of freedom need to be included. One example of a large system was presented in connection with the calculation of tunneling rate in an atomic scale system. There, the path optimization method provides an efficient way of finding the tunneling path within the so-called instanton approximation. The computational effort is similar to the widely used NEB method for finding minimum energy paths in classical systems where atomic forces from *ab initio* and density functional theory treatments of the electronic degrees of freedom are used as input. Calculations of tunneling rates using such atomic forces are not significantly harder.

An alternative approach to the implementation of the instanton approximation is to use the fact that the instanton path is a first order saddle point on the effective potential surface, V_{eff} given by equation (26), for closed Feynman paths [14]. Methods converging to first order saddle points, such as the minimum mode following method [15,16], can then be used to find tunneling paths. This approach has been used in refs. [17,18]. But, the approach presented here has several advantages over this methods. One is that the distribution of discretization points in the optimization of the JWKB tunneling path can be controlled and they can, for example, be chosen to be equally distributed while the replicas in the Feynman paths tend to cluster in the neighborhood of the end points. Also, the convergence to the saddle point has to be very tight in order to get just one negative eigenvalue. This is particularly problematic when atomic forces from electronic structure calculations are used as input. The method presented here has similar convergence properties and computational effort as the NEB

method, which is now widely used for finding classical transition paths. Finally, multiple maxima and minima on the energy surface can make the convergence to the right saddle point problematic while the calculations of the tunneling path is more robust.

It is also possible to find the optimal tunneling path by constructing an elastic band of Feynman paths, forming the so-called minimum action path, using the NEB method as was done in [14]. This, however, involves much more computation as the total number of degrees of freedom in the optimization becomes $NP(n-1)$ where P is the number of discretization points in the Feynman paths, $(n+1)$ the number of discretization points in the minimum action path and N is the number of variables in the system.

Acknowledgements. We would like to thank Judith Rommel and Johannes Kaestner for useful comments on this manuscript. This work was supported by the Icelandic Research Fund, University of Iceland research fund and EC integrated project NESSHy.

References

1. Jónsson, H., Mills, G., Jacobsen, K.W.: Classical and Quantum Dynamics in Condensed Phase Simulations. In: Berne, B.J., Ciccotti, G., Coker, D.F. (eds.), ch. 16, p. 385. World Scientific (1998)
2. Razavy, M.: Quantum Theory of Tunneling. World Scientific Publishing (2003)
3. Wigner, E.: Trans. Faraday Soc. 34, 29 (1938); Eyring, H.: J. Chem. Phys. 3, 107 (1935)
4. Vineyard, G.H.: J. Phys. Chem. Solids 3, 121 (1957)
5. Henkelman, G., Jónsson, H.: J. Chem. Phys. 113, 9978 (2000)
6. Henkelman, G., Uberuaga, B., Jónsson, H.: J. Chem. Phys. 113, 9901 (2000)
7. Rasmussen, T., Jacobsen, K.W., Leffers, T., Pedersen, O.B., Srinivasan, S.G., Jónsson, H.: Physical Review Letters 79, 3676 (1997)
8. Sheppard, D., Terrell, R., Henkelman, G.: J. Chem. Phys. 128, 134106 (2008)
9. Wilson, E.B., Decius, J.C., Cross, P.C.: Molecular Vibrations: The Theory of Infrared and Raman Vibrational Spectra. Dover (1980)
10. Callan, C.G., Coleman, S.: Phys. Rev. D 16, 1762 (1977)
11. Miller, W.H.: J. Phys. Chem. 62, 1899 (1975)
12. Messina, M., Schenter, G., Garrett, B.C.: J. Chem. Phys. 103, 3430 (1995)
13. Skodje, R.T., Truhlar, D.G.: J. Chem. Phys. 77, 5955 (1982)
14. Mills, G., Schenter, G.K., Makarov, D., Jónsson, H.: Chem. Phys. Lett 278, 91 (1997); RAW Quantum Transition State Theory. In: Berne, B.J., et al. (eds.) Classical and Quantum Dynamics in Condensed Phase Simulations, page 405. World Scientific (1998)
15. Henkelman, G., Jónsson, H.: J. Chem. Phys. 111, 7010 (1999)
16. Kaestner, J., Sherwood, P.: J. Chem. Phys. 128, 014106 (2008)
17. Arnaldsson, A.: Ph.D. thesis, University of Washington, Seattle, WA, USA (2007)
18. Andersson, S., Nyman, G., Arnaldsson, A., Manthe, U., Jónsson, H.: J. Phys. Chem. A 113, 4468 (2009)